

A multiparametric method of interpolation using WOA05 applied to anthropogenic CO₂ in the Atlantic

ANTON VELO, MARCOS VÁZQUEZ-RODRÍGUEZ, XOSE A. PADÍN,
MIGUEL GILCOTO, AÍDA F. RÍOS and FIZ F. PÉREZ

Instituto de Investigacións Mariñas (CSIC). Eduardo Cabello 6, 36208 Vigo, Spain.
E-mail: avelo@iim.csic.es

SUMMARY: This paper describes the development of a multiparametric interpolation method and its application to anthropogenic carbon (C_{ANT}) in the Atlantic, calculated by two estimation methods using the CARINA database. The multiparametric interpolation proposed uses potential temperature (θ), salinity, conservative 'NO' and 'PO' as conservative parameters for the gridding, and the World Ocean Atlas (WOA05) as a reference for the grid structure and the indicated parameters. We thus complement CARINA data with WOA05 database in an attempt to obtain better gridded values by keeping the physical-biogeochemical sea structures. The algorithms developed here also have the prerequisite of being simple and easy to implement. To test the improvements achieved, a comparison between the proposed multiparametric method and a pure spatial interpolation for an independent parameter (O_2) was made. As an application case study, C_{ANT} estimations by two methods (φC_T° and *TrOCA*) were performed on the CARINA database and then gridded by both interpolation methods (spatial and multiparametric). Finally, a calculation of C_{ANT} inventories for the whole Atlantic Ocean was performed with the gridded values and using ETOPO2v2 as the sea bottom. Thus, the inventories were between 55.1 and 55.2 Pg-C with the φC_T° method and between 57.9 and 57.6 Pg-C with the *TrOCA* method.

Keywords: CARINA, WOA05, CO₂, interpolation, multiparametric, anthropogenic carbon, back calculation.

RESUMEN: UN MÉTODO MULTIPARAMÉTRICO DE INTERPOLACIÓN UTILIZANDO WOA05, APLICADO AL CO₂ ANTROPOGÉNICO EN EL ATLÁNTICO. – Este trabajo describe el desarrollo de un método de interpolación multiparamétrico, y su aplicación al carbono antropogénico C_{ANT} en el Atlántico, calculado por dos métodos de estimación sobre la base de datos de CARINA. La interpolación multiparamétrica propuesta utiliza temperatura potencial (θ), salinidad, 'NO' y 'PO' conservativo a modo de parámetros conservativos para el mallado, y el World Ocean Atlas (WOA05) como referencia tanto para la estructura de la malla, como para los parámetros indicados. De este modo, este trabajo complementa CARINA con la base de datos de WOA05, intentando obtener mejores valores interpolados por el hecho de mantener las estructuras físico-biogeoquímicas marinas. Además, los algoritmos desarrollados tienen el prerequisite de ser sencillos y fáciles de implementar. Para comprobar las mejoras conseguidas, se ha realizado una comparación de un parámetro independiente (O_2) entre el método multiparamétrico y una interpolación puramente espacial. A modo de estudio de un caso de aplicación, se han realizado estimaciones de C_{ANT} mediante dos métodos (φC_T° and *TrOCA*) sobre la base de datos de CARINA, y posteriormente interpolado mediante ambos métodos de interpolación (espacial y multiparamétrica). Por último, se ha realizado un cálculo de los inventarios de C_{ANT} para el Océano Atlántico completo con los valores interpolados y utilizando ETOPO2v2 como fondo marino. De este modo los inventarios obtenidos fueron de entre 55.1 y 55.2 PgC con la aproximación φC_T° , y entre 57.9 y 57.6 Pg-C con la aproximación *TrOCA*.

Palabras clave: CARINA, WOA05, CO₂, interpolación, multiparamétrico, carbono antropogénico, retrocálculo.

INTRODUCTION

This work began as a contribution to the CARINA (Carbon in the Atlantic Ocean) Project, with the aim of developing an interpolation algorithm that would

enhance the gridding in low coverage areas, but with the premise of being easy to apply. The algorithm would also help to build a large and comprehensive carbon system database for the Atlantic Ocean with the CARINA database. The development should con-

tribute to estimate the C_{ANT} inventory of this ocean by, as part of a future work, gridding the C_{ANT} that can be calculated with the available approximation methods. Finally, the interpolation method could be used in the CARINA project to help to get the gridded product from the other available CARINA parameters. The interpolation algorithms developed here pursue the goal of being simple and easy to implement. After the seminal work of Gandin (1965) introducing objective analysis to produce gridded maps of meteorological variables in a systematic manner, objective interpolation methods were transferred from meteorology to oceanography in the late 1970s (Bretherton *et al.*, 1976; Freeland and Gould, 1976; Jalickee and Hamilton, 1977). Today, objective analysis appears in standard oceanography texts such as Bennett (1992) and Emery and Thomson (2001). In fact, one of the databases used in the present study, the World Ocean Atlas (WOA05, see Material and Methods section), was processed with these data analysis techniques. The present study uses a multiparametric inverse distance algorithm that was applied to the CARINA data (see the Material and Methods section) and took the WOA05 objective interpolated data as a reference to calculate the multiparametric distances. This approach provides a simple interpolation algorithm that is easy to use and to quality assess.

The CARINA Project has fed its dataset only from cruises in which carbon parameters were measured, so data coverage is low in certain regions, such as the Southern Ocean. Within this context, an interpolation method based only on geographical distances might perform poorly precisely on these regions due to the sparseness. A possible way to alleviate this problem is to incorporate more information in the interpolation algorithm other than the spatial. Thus, the consideration of fields of conservative properties for different water masses would become a benefit in this regard, providing better fits to real distributions than those generated from a purely spatial distance-based method. One additional advantage of this procedure is that the artefacts that may appear in the water mass distributions derived from plain spatial interpolations could be avoided.

The CARINA dataset is not distributed over a structured uniform grid, but is rather composed mainly from dispersed CTD stations organized in transoceanic sections. In terms of recorded variables, the dataset compiles many biogeochemical parameters, including the ones needed for the calculation of C_{ANT} by different methods. In contrast, the WOA05 dataset is structured in a homogenous three dimensional grid with thermohaline and biogeochemical variables defined at the nodes of the grid, but it lacks many of the parameters needed for carbon calculations. Therefore, the generation of a multiparametric interpolation algorithm that combines the properties of the WOA05 and CARINA datasets appears to be the logical way to proceed. Applying this to C_{ANT} es-

timation should provide C_{ANT} interpolated data over the structured WOA05 grid, taking advantage of the common hydrographical information available in both datasets.

As a way to evaluate the results, two versions of the interpolation method were compared; one based only on spatial distances and one that uses the physical and biogeochemical tracers (hereafter referred to as the Water Mass Properties [*WMP*] interpolation method). The contrast of the individual behaviour of the two methods was carried out using dependent variables (interpolating variables included in the multiparametric distances) and one independent variable (oxygen, not included in the multiparametric distances).

As the quality tests of the *WMP* interpolation method yield positive results, a step forward was taken: interpolating anthropogenic carbon over the WOA05 grid. The major role played by the oceans in the global carbon cycle is incontrovertible, since they have the capacity to sequester 2.2 ± 0.4 Pg C per year, roughly a 25% of the total anthropogenic carbon (C_{ANT}) emitted to the atmosphere (8.0 ± 0.5 Pg yr⁻¹) (Canadell *et al.*, 2007). Most outstandingly, the Atlantic Ocean stores 38% of the oceanic anthropogenic carbon (Sabine *et al.*, 2004), though it represents 29% of the global ocean surface area. The particular dynamics of the Atlantic Ocean allows the formation of deep waters in the North Atlantic and this enhances the uptake fluxes and storage capacity of C_{ANT} of this basin. Recently detected processes triggered by decadal changes of global climate, such as the slowdown of the Meridional Overturning Circulation, seem to have contributed significantly to reducing the sink capacity of C_{ANT} in both the North Atlantic and the Southern Ocean (Joos *et al.*, 1999; Le Quéré *et al.*, 2007). The juxtaposition of these opposed effects has dramatically magnified the need to accurately estimate the state of C_{ANT} inventories and has raised the importance of fine-tuning the C_{ANT} interpolation methods applied to sparse or geographically disperse datasets.

Two methods were used to obtain the estimation of C_{ANT} over the whole Atlantic Ocean, φC_T° and *TrOCA*. The φC_T° estimation method was chosen as it was developed by the authors (Vázquez-Rodríguez *et al.*, 2009a) and it was straightforward to apply and verify (the MATLAB script is publicly available for download at <http://oceanio.iim.csic.es/co2group/>). It is also an updated method and seems to perform well in comparison with other methods (Vázquez-Rodríguez *et al.*, 2009b). The *TrOCA* method (Touratier *et al.*, 2007) was additionally considered as a support reference due to its ease of application. Consequently, anthropogenic carbon was calculated by applying these estimations to the CARINA dataset, and then gridded by both the *WMP* and *Spatial* interpolation methods. The next step taken was to calculate the volumes in order to obtain the inventories. ETOPO2v2 (U.S. Department of Commerce, 2006) was chosen as reference for the ocean floor in these calculations.

MATERIALS AND METHODS

Database

CARINA is a database of comprehensive carbon data, sourced from hydrographic cruises conducted in the Arctic, Atlantic and Southern Oceans. The project was initiated in 1999 as an essentially informal and unfunded project in Kiel, Germany, with the main goal of creating a database of relevant carbon variables to be used for accurate assessments of carbon inventories, transports and uptake rates. The CARINA data have been gathered from various sources and then put under rigorous quality controls (QC) to produce a consistent data product. Experience with previous synthesis efforts like the Global Data Analysis Project (GLODAP) (Key *et al.*, 2004) demonstrated that a consistent data product can be achieved from different cruises, performed by different laboratories and in very different regions. The CARINA database includes data and metadata from 188 oceanographic cruises or projects, (Hoppema *et al.*, 2009; Tanhua *et al.*, 2009; Key *et al.*, 2010; Tanhua *et al.*, 2010). In addition, 52 WOCE/GLODAP cruises were included in the quality control to ensure consistency with historical data. Parameters included in the CARINA dataset are salinity (S), potential temperature (θ), oxygen (O_2), nitrate (NO_3), phosphate (PO_4), silicate (SiO_4), total alkalinity (A_T), fugacity of carbon dioxide (fCO_2), total inorganic carbon (C_T), pH, CFC-11, CFC-12, CFC-113 and CCl_4 . Due to the different origins of the data, the data density has heterogeneous distributions, being scarcer in the South Atlantic than in the North Atlantic.

The World Ocean Atlas 2005 (WOA05) has widely proven its usefulness to the oceanographic and atmospheric research communities. WOA05 offers a gridded database interpolated from many different sources by oceanographic objective analysis techniques. The WOA05 climatological analyses were carried out on a $1^\circ \times 1^\circ$ grid. This comes from the fact that higher resolution analyses are not justified for all the measured properties, and they should be analyzed in the same manner. For a description of the WOA05 data and statistical fields, refer to <http://www.nodc.noaa.gov/OC5/WOA05/pubwoa05.html>. The site includes a list of values and statistical data in a one-degree latitude-longitude world grid (360×180) at 33 standard depth levels from the surface to a maximum depth of 5500 m.

The WOA05 series include analysis of temperature (Locarnini *et al.*, 2006), salinity (Antonov *et al.*, 2006), dissolved oxygen, apparent oxygen utilization, oxygen saturation (Garcia *et al.*, 2006a), and dissolved inorganic nutrients (Garcia *et al.*, 2006b). The climatologies defined here come from historical oceanographic profiles and selected data at different depths. Data used in the WOA05 were analyzed in a consistent, objective analysis mode and interpolated over a one-degree latitude-longitude grid at standard depth levels.

The aim of the WOA05 maps is to illustrate the large-scale characteristics of the distribution of ocean temperature. The fields used to generate these climatological maps were computed by objective analysis of quality-controlled historical temperature data. Maps are presented for climatological composite periods (annual, seasonal, monthly, and monthly difference fields from the annual mean field, and the number of observations) at selected standard depths. The annual climatology was calculated using all data regardless of the month of the observation. Seasonal climatologies were calculated using only data from the defined season (regardless of year). However, in this study only the annual maps for the whole Atlantic Ocean (Lat: $90^\circ S$ - $90^\circ N$, Lon: $81^\circ W$ - $33^\circ E$) were used.

For the C_{ANT} inventory calculations, the ETOPO2v2 (USDC, NOAA, NGDC 2006) bathymetry was used as bottom reference to calculate the volume of the deepest boxes.

Interpolation Method

Hereafter *var* is the parameter that we wish to interpolate. The objective is to obtain for each node j of the structured WOA05 grid an average value of *var*, which is unavailable from this database. The known values of *var* from the CARINA unstructured-grid nodes i will be used to fill in the j WOA05 nodes. A classic interpolation scheme of inverse distance is applied, using a weighted estimation of the i neighbouring samples to the j WOA05 node:

$$\text{var}_j = \frac{\sum_i \text{var}_i (f_i^j)^{-1}}{\sum_i (f_i^j)^{-1}} \quad (1)$$

The weighting factors used in the basic spatial interpolation are defined by:

$$\begin{aligned} f_i^j = & w_{lat} \left(\frac{lat^i - lat^j}{\Delta lat} \right)^2 + w_{lon} \left(\frac{lon^i - lon^j}{\Delta lon} \right)^2 + \\ & + w_z \left(\frac{z^i - z^j}{\Delta z} \right)^2 + w_\theta \left(\frac{\theta^i - \theta^j}{std(\theta^j)} \right)^2 + w_S \left(\frac{S^i - S^j}{std(S^j)} \right)^2 + \\ & + w_{NO} \left(\frac{NO^i - NO^j}{std(NO^j)} \right)^2 + w_{PO} \left(\frac{PO^i - PO^j}{std(PO^j)} \right)^2 \end{aligned} \quad (2)$$

where several variables are pondered with arbitrary weights (w_x). The specific values of the w_x terms to produce the f_i^j factors are subjected to the criteria of the researcher. The information concerning the geographical position is taken into account in the interpolation through the spatial coordinates of longitude (lon), latitude (lat) and depth (z). The interpolation factors are also determined using the information from four tracers: salinity (S), potential temperature (θ), 'NO'

and 'PO'. Both 'NO' ($=9[\text{NO}_3]+[\text{O}_2]$) and 'PO' ($=135[\text{HPO}_4]+[\text{O}_2]$) are conservative parameters, and like *potential temperature* and *salinity* they are characteristic of each water mass (Broecker, 1974; Ríos *et al.*, 1989; Pérez *et al.*, 1993). The Δlat , Δlon and Δz appearing in Equation (2) are the intervals of latitude, longitude and depth. Three different intervals were taken as results of sample availability in the CARINA database. First, a $\pm 2^\circ \times \pm 2^\circ$ (Lat-Lon) window was used. A larger area of $\pm 10^\circ \times \pm 10^\circ$ (Lat-Lon) was chosen if fewer than 20 samples were found in the previous boundary, and if again no samples were found within this interval, then the boundaries were expanded to an even bigger window of $\pm 20^\circ \times \pm 20^\circ$ (Lat-Lon). For depth, an interval of $\pm(150 + 0.1 \times \text{depth})$ metres was used. The tracer (S , θ , NO and PO) differences between the WOA05 and CARINA nodes are normalized using the standard deviation from each tracer computed in the corresponding equivalent volume defined by the intervals of latitude, longitude and depth. The quotient terms of the spatial or tracer differences with their spatial intervals or tracer standard deviations are then squared to convert them into the classical inverse quadratic distance interpolation equation.

Two different kinds of interpolations were applied to produce three-dimensional O_2 and C_{ANT} fields. The first one is designated as the "spatial interpolation" and is defined from the following weights:

$$w_{\text{lat}} w_{\text{lon}} w_z w_\theta w_S w_{NO} w_{PO} = (1, 1, 1, 0, 0, 0, 0) \quad (3)$$

These factors avoid the influence of the tracer properties in the interpolation. On the other hand, the "WMP interpolation" stands for the interpolation without weights in the spatial coordinates (latitude, longitude and depth) and using only the tracer variables:

$$w_{\text{lat}} w_{\text{lon}} w_z w_\theta w_S w_{NO} w_{PO} = (0, 0, 0, 1, 1, 1, 1) \quad (4)$$

C_{ANT} estimation methods

Two recently developed C_{ANT} back-calculation methods, φC_T° and $TrOCA$, were selected to determine C_{ANT} in the present study. Both methods separate the contributions to total carbon (C_T) from organic matter remineralization and CO_3Ca dissolution in a similar mode. However, there are characteristic distinctions. The $TrOCA$ method uses a constant Redfield ratio (R_C) value of 1.35 (Kortzinger *et al.*, 2001), while the φC_T° method, following the ΔC^* method, uses the constant R_C ratio (1.45) proposed by Anderson and Sarmiento (1994). The most important difference between the two methods, though, lies in the way the reference for C_{ANT} -free waters is obtained. The $TrOCA$ method estimates C_{ANT} using the following simple relationship:

$$C_{ANT} = \frac{(TrOCA - TrOCA^0)}{a} \quad (5)$$

where $TrOCA$ represents a quasi-conservative tracer calculated from O_2 , C_T and A_T as follows:

$$TrOCA = \text{O}_2 + a (C_T - 0.5 A_T) \quad (6)$$

The $TrOCA^0$ reference represents the $TrOCA$ tracer without any anthropogenic carbon influence, i.e. the pre-industrial $TrOCA$:

$$TrOCA^0 = e^{b+c\theta+\frac{d}{A_T^2}} \quad (7)$$

The coefficients a , b , c and d in the above equations are properly defined and established in Touratier *et al.* (2007). The $TrOCA^0$ equation is obtained from $\Delta^{14}\text{C}$ and $CFC-11$ data in the global ocean. The $\Delta^{14}\text{C}$ data are used to establish which water parcels can be assumed to be free of C_{ANT} . When the concentration of $\Delta^{14}\text{C} < 175\text{‰}$, the age of the corresponding water mass is greater than 1400 years, long before the massive emissions of CO_2 by humans had begun. The samples with maximum $CFC-11$ concentrations, typically between 262.9 and 271.3 pptv and corresponding to surface waters in 1992-1995 (maximum atmospheric $pCFC-11$), were also selected as part of the dataset to obtain the $TrOCA^0$ expression. Touratier *et al.* (2007) estimated an uncertainty of $\pm 6.2 \mu\text{mol kg}^{-1}$ in C_{ANT} determination for the $TrOCA$ method, using an error propagation technique as in numerous previous studies (Gruber *et al.*, 1996; Sabine *et al.*, 1999).

The φC_T° method (Vázquez-Rodríguez *et al.*, 2009a) shares similar fundamentals with the ΔC^* back-calculation method (Lee *et al.*, 2003). The sub-surface layer (100-200 m) is taken in the φC_T° method as a reference for characterizing water mass properties at the moment of their formation. The air-sea CO_2 disequilibrium (ΔC_{dis}) is parameterized at the sub-surface layer first using a short-cut method (Thomas and Ittekkot, 2001) to estimate C_{ANT} . Since the average age of the water masses in the 100-200 m depth domain, and most importantly in outcropping regions it is under 25 years, the use of the short-cut method to estimate C_{ANT} is appropriate (Matear *et al.*, 2003). The pre-industrial total alkalinity A_T° and ΔC_{dis} parameterizations (in terms of conservative tracers) obtained from sub-surface data are applied directly to calculate C_{ANT} in the water column for waters above the 5°C isotherm and via an Optimum MultiParameter analysis (OMP) for waters with $\theta < 5^\circ\text{C}$. This procedure especially improves the estimates in cold deep waters that are subject to strong and complex mixing processes between Arctic and Antarctic water masses. Waters below the 5°C isotherm also represent an enormous volume of the global ocean ($\sim 86\%$). One important aspect of the φC_T° method is that none of the A_T° or ΔC_{dis} parameterizations are CFC -reliant. In addition, the φC_T° method proposes an approximation to the temporal and spatial variability of ΔC_{dis} ($\Delta\Delta C_{dis}$) in the Atlantic Ocean in terms of C_{ANT} and

ΔC_{dis} itself. Also, the small increase in A_T° since the Industrial Revolution due to CaCO_3 dissolution changes projected from models (Heinze, 2004), and the effect of rising sea surface temperatures on the parameterized A_T° are accounted for in the parameterizations. These two last corrections are minor but should still be considered if one wished to avoid a maximum $4 \mu\text{mol kg}^{-1}$ bias ($2 \mu\text{mol kg}^{-1}$ on average) in C_{ANT} estimates. The φC_T° method expression for the calculation of C_{ANT} is as follows:

$$C_{ANT} = \frac{\Delta C^* - \Delta C_{dis}^t}{1 + \varphi \frac{|\Delta C_{dis}^t|}{C_{ANT}^{sat}}} \quad (8)$$

The ΔC^* method is defined after Gruber *et al.* (1996) as:

$$\Delta C^* = C_T - \frac{AOU}{R_c} - 0.5(PA_T - PA_T^0) - C_T^{\pi_{eq}} \quad (9)$$

The constant term φ is a proportionality factor that stands for the $\Delta C_{dis} / \Delta C_{dis}^t$ ratio and its value (0.55) is properly discussed in Vázquez-Rodríguez *et al.* (2009a). The ΔC_{dis}^t and PA_T^0 terms are parameterized as a function of conservative parameters exclusively (Vázquez-Rodríguez *et al.*, 2009a). The C_{ANT}^{sat} stands for the theoretical C_{ANT} saturation concentration depending on the $p\text{CO}_2$ at the time of water masses formation (WMF), and is defined as $C_{ANT}^{sat} = S/35 (0.85\theta + 46.0)$ (at present $x\text{CO}_2$ air). Based on earlier uncertainty and error evaluations (Gruber *et al.*, 1996; Sabine *et al.*, 1999; Lee *et al.*, 2003; Touratier *et al.*, 2007), an estimated overall uncertainty of $\pm 5.2 \mu\text{mol kg}^{-1}$ is obtained for the φC_T° method. This is in agreement with the av-

TABLE 1. – Mean and standard deviation (STD) of the interpolated data minus WOA05 data are computed for the whole Atlantic, for specific sub domains and for the spatial and WMP interpolation. The determination coefficient (r^2) between WOA05 and interpolated fields is also provided. Temperature is in $^\circ\text{C}$, Salinity in psu and NO , PO and O_2 in $\mu\text{mol kg}^{-1}$.

| Total | r^2 | Total Mean | Std | r^2 | $\theta > 5^\circ\text{C}$ Mean | Std | r^2 | $\theta < 5^\circ\text{C}$ Mean | Std |
|----------------------|-------|------------|------|-------|---------------------------------|------|-------|---------------------------------|------|
| θ spatial | 0.964 | 0.34 | 1.02 | 0.856 | 0.23 | 0.62 | 0.914 | 0.55 | 1.48 |
| θ WMP | 0.993 | 0.10 | 0.43 | 0.952 | 0.11 | 0.37 | 0.988 | 0.07 | 0.53 |
| Sspatial | 0.925 | 0.01 | 0.14 | 0.887 | -0.02 | 0.07 | 0.905 | 0.04 | 0.22 |
| SWMP | 0.984 | 0.00 | 0.07 | 0.954 | -0.01 | 0.05 | 0.981 | 0.00 | 0.09 |
| NOspatial | 0.948 | 0.8 | 18.8 | 0.845 | 3.8 | 15.5 | 0.918 | -4.7 | 22.7 |
| NOWMP | 0.989 | 2.5 | 8.6 | 0.957 | 3.6 | 8.2 | 0.983 | 0.4 | 9.2 |
| POspatial | 0.956 | -5.7 | 18.6 | 0.893 | -4.3 | 15.3 | 0.919 | -8.2 | 23.2 |
| POWMP | 0.991 | -3.0 | 8.4 | 0.971 | -3.1 | 8.1 | 0.984 | -2.7 | 8.7 |
| O_2 spatial | 0.901 | 4.1 | 14.5 | 0.857 | 4.4 | 13.1 | 0.918 | 3.7 | 16.6 |
| O_2 WMP | 0.943 | 2.6 | 11.0 | 0.945 | 2.7 | 8.4 | 0.921 | 2.6 | 15.0 |
| Lat > 30°N | | | | | | | | | |
| θ spatial | 0.934 | 0.20 | 1.24 | 0.860 | 0.34 | 1.61 | 0.80 | 0.01 | 0.42 |
| θ WMP | 0.987 | 0.06 | 0.55 | 0.987 | 0.06 | 0.55 | 0.82 | 0.04 | 0.41 |
| Sspatial | 0.832 | 0.02 | 0.20 | 0.752 | 0.03 | 0.27 | 0.72 | 0.00 | 0.06 |
| SWMP | 0.948 | 0.01 | 0.11 | 0.948 | 0.01 | 0.11 | 0.87 | 0.01 | 0.09 |
| NOspatial | 0.954 | -1.0 | 12.7 | 0.916 | -3.6 | 15.7 | 0.64 | 2.3 | 6.3 |
| NOWMP | 0.988 | 0.7 | 6.6 | 0.988 | 0.7 | 6.6 | 0.82 | 2.4 | 4.3 |
| POspatial | 0.937 | -5.1 | 15.6 | 0.877 | -6.3 | 19.6 | 0.57 | -3.6 | 8.2 |
| POWMP | 0.988 | -2.2 | 7.0 | 0.988 | -2.2 | 7.0 | 0.82 | -1.6 | 4.8 |
| O_2 spatial | 0.928 | 0.6 | 9.3 | 0.875 | 0.1 | 11.2 | 0.88 | 1.1 | 6.1 |
| O_2 WMP | 0.946 | -0.6 | 8.2 | 0.946 | -0.6 | 8.2 | 0.91 | 0.5 | 5.4 |
| Tropical | | | | | | | | | |
| θ spatial | 0.982 | 0.30 | 0.83 | 0.958 | 0.59 | 1.11 | 0.985 | 0.03 | 0.14 |
| θ WMP | 0.998 | 0.06 | 0.27 | 0.995 | 0.11 | 0.38 | 0.994 | 0.02 | 0.08 |
| Sspatial | 0.956 | 0.01 | 0.12 | 0.943 | 0.03 | 0.17 | 0.981 | -0.01 | 0.02 |
| SWMP | 0.995 | 0.00 | 0.04 | 0.994 | 0.00 | 0.06 | 0.993 | 0.00 | 0.01 |
| NOspatial | 0.981 | 1.6 | 11.0 | 0.968 | -1.7 | 13.6 | 0.898 | 4.7 | 6.3 |
| NOWMP | 0.995 | 2.5 | 5.3 | 0.992 | 1.8 | 6.6 | 0.964 | 3.2 | 3.8 |
| POspatial | 0.979 | -2.2 | 11.6 | 0.967 | -5.1 | 13.4 | 0.858 | 0.6 | 8.6 |
| POWMP | 0.995 | -1.0 | 5.7 | 0.992 | -1.6 | 6.5 | 0.955 | -0.5 | 4.8 |
| O_2 spatial | 0.926 | 5.7 | 14.1 | 0.83 | 8.0 | 19.0 | 0.970 | 3.5 | 5.8 |
| O_2 WMP | 0.937 | 5.7 | 12.8 | 0.86 | 6.6 | 17.2 | 0.963 | 4.8 | 6.5 |
| Lat < 30°S | | | | | | | | | |
| θ spatial | 0.92 | 0.44 | 1.05 | 0.82 | 0.77 | 1.93 | 0.74 | 0.38 | 0.75 |
| θ WMP | 0.983 | 0.14 | 0.47 | 0.97 | -0.04 | 0.66 | 0.92 | 0.17 | 0.43 |
| Sspatial | 0.77 | 0.00 | 0.13 | 0.82 | 0.09 | 0.22 | 0.75 | -0.02 | 0.09 |
| SWMP | 0.96 | -0.01 | 0.05 | 0.97 | -0.01 | 0.09 | 0.94 | -0.01 | 0.05 |
| NOspatial | 0.82 | 0.9 | 24.9 | 0.82 | -13.5 | 39.9 | 0.53 | 3.7 | 19.5 |
| NOWMP | 0.96 | 3.4 | 11.1 | 0.96 | -1.2 | 15.5 | 0.86 | 4.0 | 10.1 |
| POspatial | 0.85 | -8.7 | 23.2 | 0.83 | -18.2 | 38.5 | 0.65 | -6.8 | 18.2 |
| POWMP | 0.97 | -4.9 | 10.1 | 0.97 | -5.8 | 13.2 | 0.90 | -4.8 | 9.5 |
| O_2 spatial | 0.75 | 4.4 | 16.3 | 0.78 | -1.4 | 14.5 | 0.73 | 5.6 | 16.3 |
| O_2 WMP | 0.91 | 1.7 | 9.8 | 0.83 | -1.7 | 11.4 | 0.92 | 2.1 | 9.4 |

erage uncertainty of $5.6 \mu\text{mol kg}^{-1}$ for ΔC_{dis} (Vázquez-Rodríguez *et al.*, 2009a).

For the application case of C_{ANT} interpolation ($var = C_{ANT}$ in equation 1) the computed C_{ANT} must be normalized to a reference year (1994) using the following expression:

$$C_{ANT,i}^{1994} = \frac{C_{ANT}^{sat,1994}}{C_{ANT}^{sat,year}} C_{ANT,i}^{year} \quad (10)$$

The reason for doing this comes from the transient tracer nature of C_{ANT} and the fact that the CARINA database spans quite a long time period. Therefore, the interpolated C_{ANT} referenced to 1994 (C_{ANT}^{1994}) is computed as

$$C_{ANT}^{1994} = \frac{\sum_i C_{ANT,i}^{1994} (f_i^j)^{-1}}{\sum_i (f_i^j)^{-1}} \quad (11)$$

which is valid for both C_{ANT} reconstruction methods.

RESULTS AND DISCUSSION

To assess the quality of both types of interpolation, their results were evaluated against the WOA05 data, i.e. the interpolated *potential temperature*, *salinity*, *'NO'* and *'PO'* obtained from equation (1) were compared with the corresponding original values from WOA05 variables. Since these parameters were involved in factor's calculation of the WMP interpolation (Eqs. 2, 4), a more independent check was done by interpolating O_2 and comparing it against the WOA05

O_2 data. When the interpolation methods had been assessed, they were applied to C_{ANT} , using both φC_T° and *TrOCA* methods, in order to get the 3D distribution and the total inventories.

The mean and standard deviation (STD) of the interpolated data minus the reference WOA05 data (S , θ , *'NO'*, *'PO'* and O_2) were computed for the whole domain and for specific sub-domains (Table 1). Also, the correlation between interpolated and reference fields was characterized with the determination coefficient (r^2). Three zones were selected depending on the general variability of water masses, namely: northern latitudes (lat $>30^\circ\text{N}$), tropical latitudes and southern latitudes (lat $<30^\circ\text{S}$). In addition, two depth levels were set with respect to the 5°C isotherms: $\theta >5^\circ\text{C}$ and $\theta <5^\circ\text{C}$. The 5°C isotherm represents a coarse boundary between the little-ventilated deep waters and the younger, more ventilated upper and intermediate waters. It also splits the C_{ANT} inventories in about half.

The climatological annual mean of WOA05 potential temperature along the 28°W section in WOA05 (Fig. 1) is shown in Figure 2A. The spatially-interpolated potential temperature ($\theta_{spatial}$) from the CARINA data base is close to the WOA05 data (Fig. 2B). However, some misfits do show up when the residuals are plotted (Fig. 2D). The larger residuals are located in the upper layer, where absolute values higher than 2°C are reached. In the deep water there is a better agreement, although southward of 40°S there is a large thick layer holding a systematic bias, higher than 1°C . On the other hand, the potential temperature

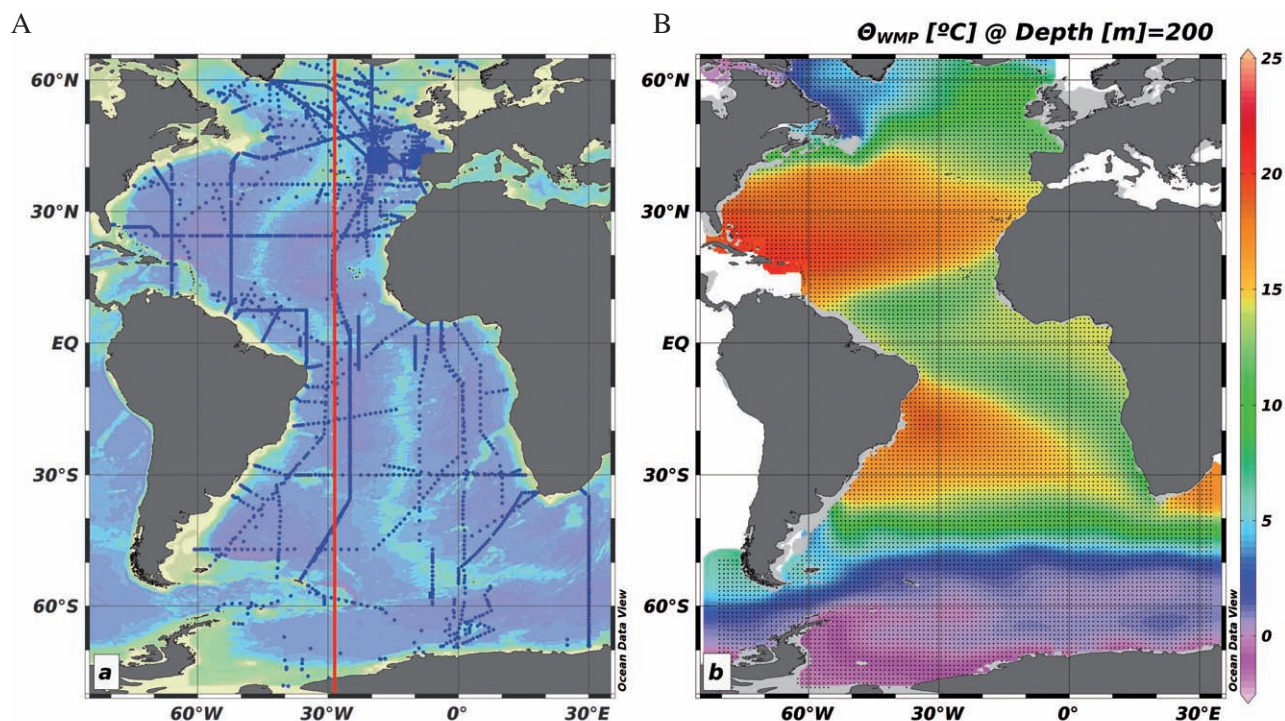


FIG. 1. – A, CARINA stations with available variables needed to estimate C_{ANT} and section 28°W plotted. B, WOA05 data grid sample with θ ($^\circ\text{C}$).

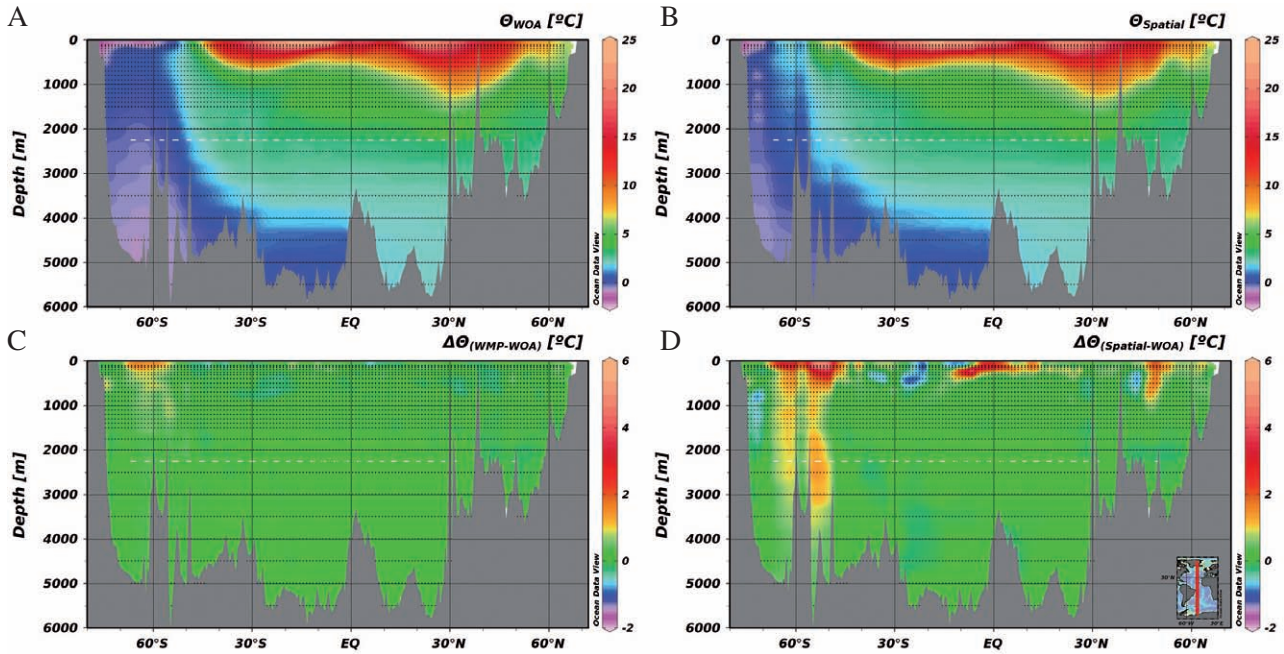


Fig. 2. – Potential temperature (°C) variability along 28°W from the WOA05 dataset (A), spatially interpolated from CARINA data (B). Residuals of WMP interpolated (C) and spatially interpolated (D) potential temperature both as interpolated minus WOA05.

from the *WMP* interpolation (θ_{WMP}) (Fig. 2C) shows a better agreement and lower residuals than the spatial interpolation. This time, as for $\theta_{spatial}$, the best fit is found in deep waters, north of 45°S. Statistically speaking, the best fit (Table 1) is obtained by the *WMP* interpolation irrespective of whether the whole Atlantic is included or the interpolation is restricted to the sub-domains previously defined. The largest

differences between the two kinds of interpolation are located in the upper layer ($\theta > 5^\circ\text{C}$), where r^2 increases noticeably when the *WMP* interpolation is used. More specifically, the best fits are obtained in the tropical region and northern latitudes, whereas the southern latitudes show the worst fits. This is probably due to the lower density of data that the CARINA database has in the Southern Ocean.

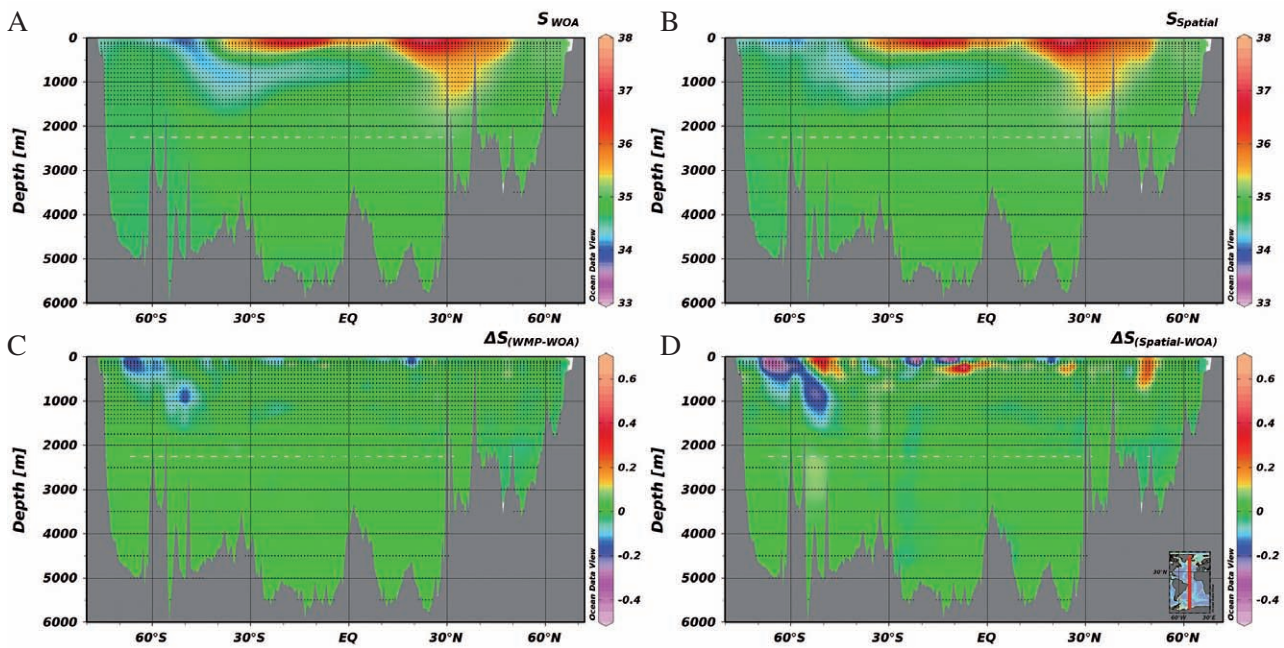


Fig. 3. – Salinity variability along 28°W from the WOA05 dataset (A), spatially interpolated from CARINA data (B). Residuals of WMP interpolated (C) and spatially interpolated (D) salinity, both as interpolated minus WOA05.

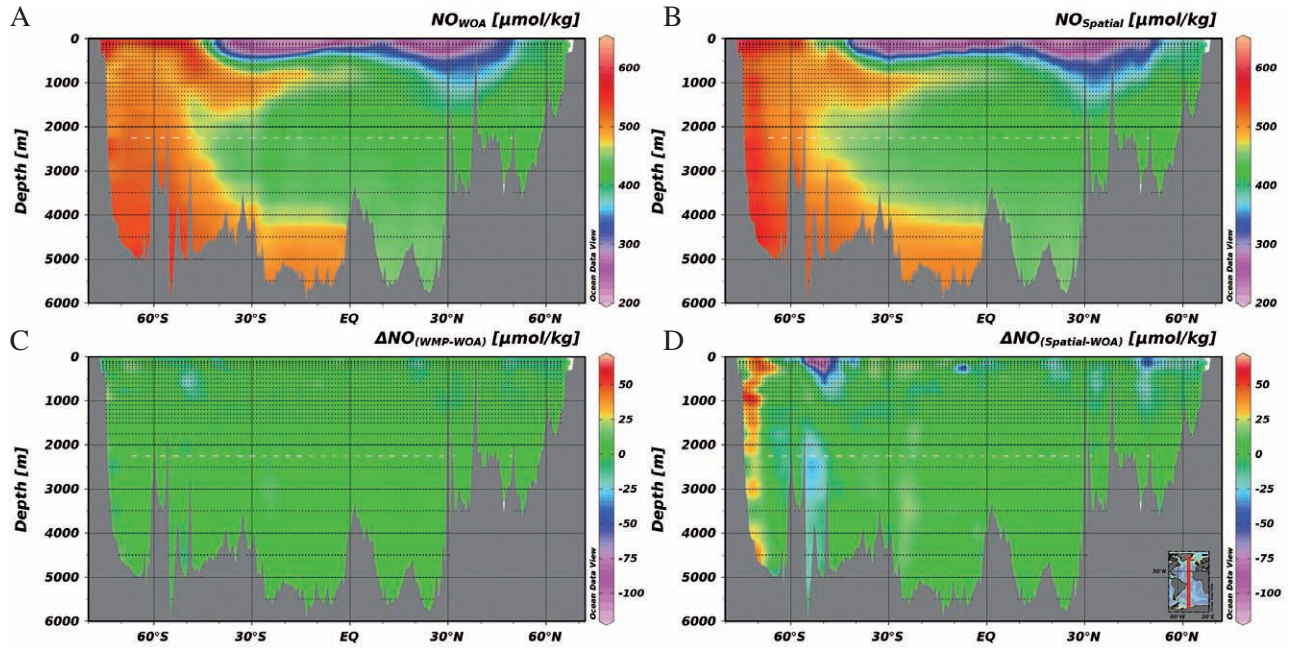


FIG. 4. – NO ($\mu\text{mol kg}^{-1}$) variability along 28°W from the WOA05 dataset (A), spatially interpolated from CARINA data (B). Residuals of WMP interpolated (C) and spatially interpolated (D) NO, both as interpolated minus WOA05.

Figure 3A shows the WOA05 climatological annual mean of salinity along the vertical section defined by the 28°W meridian (Fig. 1). As in the case of $\theta_{spatial}$, the spatially interpolated salinity ($S_{spatial}$) from the CARINA database is quite close to the WOA05 reference data (Fig. 3B). Some misfits can be observed when the residuals between the spatially interpolated and WOA05 salinity values are plotted for the 28°W section (Fig. 3D). For instance, there is a considerable error

located around the salinity minimum associated with the presence of Antarctic Intermediate Water (AAIW) (Mémery *et al.*, 2000). Again, the greater residuals are found in the upper layers where absolute values higher than 0.2 psu are observed. Although in the deep waters the concordance is high in general, south of 40°S there is still the same thick layer of large biases (higher than 0.05 psu in this case) also observed with the $\theta_{spatial}$. The WMP interpolation of salinity (S_{WMP}) (Fig. 3C) shows

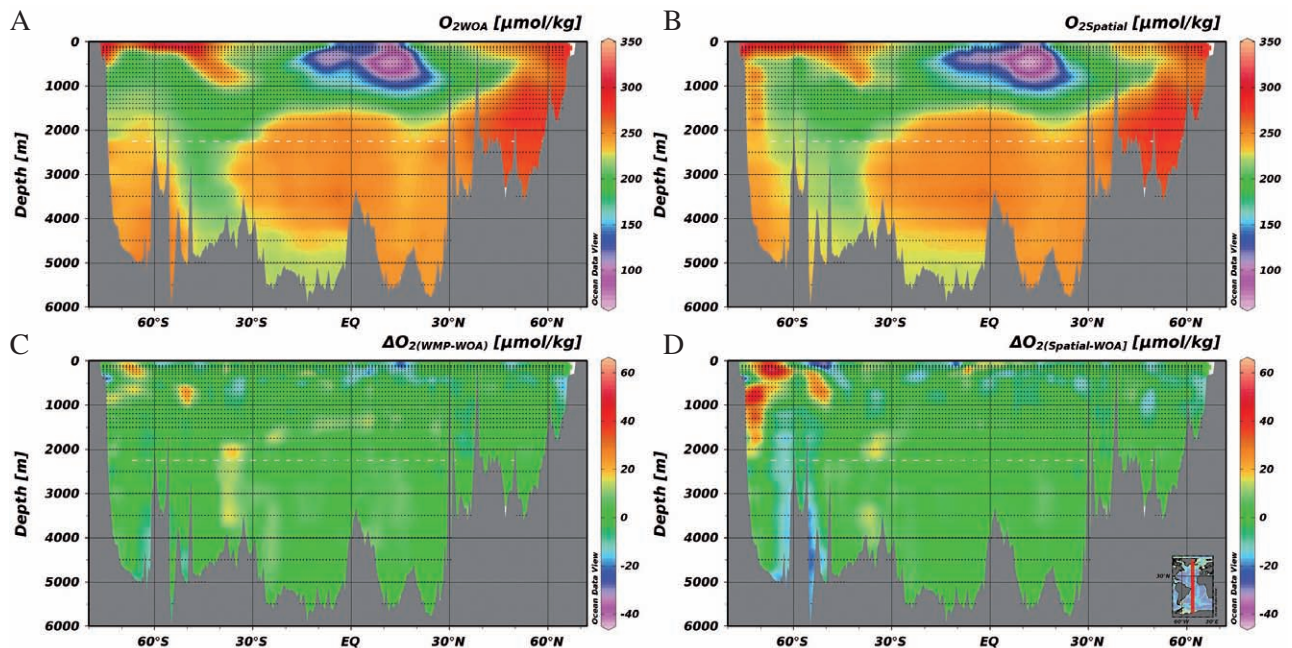


FIG. 5. – O₂ ($\mu\text{mol kg}^{-1}$) variability along 28°W from the WOA05 dataset (A), spatially interpolated from CARINA data (B). Residuals of WMP interpolated (C) and spatially interpolated (D) O₂, both as interpolated minus WOA05.

better agreement and lower residuals than the $S_{spatial}$ interpolation in all sub-domains (Table 1), proving again a superior performance of the *WMP* over the purely spatial interpolation method. Generally, both interpolation methods seem to perform better for salinity in the deep waters north of 45°S (Fig. 3D). Quantitatively speaking, the best fit to WOA05 values is obtained by the *WMP* interpolation in the tropical region (Table 1). The largest discrepancies between results from the two interpolation algorithms are found in the upper layers ($\theta > 5^\circ\text{C}$) of North Atlantic waters. Here, the r^2 obtained with the *WMP* algorithm are better by far than the ones produced by the spatial approach. However, the r^2 values obtained for S are generally slightly lower than those of θ .

The climatological annual mean of 'NO' is shown along 28°W (Fig. 4A). Since 'NO' and 'PO' are highly correlated, the 'PO' fields are not shown for the sake of conciseness. The spatial interpolation of 'NO' ($NO_{spatial}$) is close to the WOA05 data (Fig. 4B), with a most noteworthy r^2 of 0.948 (Table 1) for the whole Atlantic. The upper layers of the ocean, and particularly the Southern Ocean (SO), display the largest anomalies, which exceptionally reach offsets of 50 $\mu\text{mol kg}^{-1}$ (Fig. 4D). In general, the NO_{WMP} output shows better agreement, lower standard deviations in residuals and higher determination coefficients than the $NO_{spatial}$ in every subdomain (Table 1). Unlike the θ case, the best fit is found in the upper warm layers of the Atlantic Ocean rather than in the deep ones. This is likely due to the relatively high variability of 'NO' observed in the upper layer. Conversely, the worst fit (lowest r^2), is found in the deep layers of the Southern Ocean.

The interpolated oxygen fields can be used as a test to assess the quality of the interpolation from CARINA data, given that this variable is common to both datasets and it is not used in the interpolation algorithms. The concentration of oxygen is controlled by the biological and solubility pumps. The climatological annual mean of O_2 along the 28°W section (Fig. 5A) exhibits a strong minimum in the upper layer in the tropical region caused by the remineralization of organic matter (biological pump predominance). The high values observed in the polar areas are the consequence of the high solubility of oxygen in cold surface waters (solubility pump prevails the biological processes). The spatially interpolated O_2 ($O_{2spatial}$) (Fig. 5B) closely resembles the WOA05 O_2 distribution along the 28°W vertical section (Fig. 5A). It is generally well correlated (r^2 of 0.90, Table 1) in the Atlantic Ocean, though the purely-spatial interpolation has a slight tendency to over-spline some O_2 gradients in the southern latitudes. The largest differences and lowest correlations between the observed and the $O_{2spatial}$ fields are located in the upper Atlantic layer (ranging from -25 to 20 $\mu\text{mol kg}^{-1}$) and in the Southern Ocean, where offsets may reach up to 50 $\mu\text{mol kg}^{-1}$ (Fig. 5D). The best fits obtained belong to the cold deep layers of the tropical region.

The O_2 *WMP* interpolation (O_{2WMP}) (Fig. 5C) is in better agreement with direct observations, has lower residuals (Fig. 5C) and has higher r^2 in general than the spatial interpolation (r^2 of 0.94 vs. r^2 of 0.90 respectively, Table 1). Unlike for the rest of domains, in deep tropical waters the *WMP* interpolation seems not to perform up to its potential, as the results from the spatial interpolation appear to be more in accordance with the observed fields. Most importantly, the *WMP* interpolation algorithm yields robust estimates in the Southern Ocean, where data coverage of the CARINA database is rather sparse.

As C_{ANT} is indistinguishable from natural CO_2 , there are no C_{ANT} benchmarks against which the estimations can be compared. Figure 6 shows the spatial and *WMP* interpolations of C_{ANT} computed using the φC_T° method. The general pattern of the distributions is similar to those given by Lee *et al.* (2003) and Vázquez-Rodríguez *et al.* (2009b). Sabine *et al.* (2004), using GLODAP gridded database, produced a total inventory of C_{ANT} for the Atlantic of 40 Pg-C. Previously, Lee *et al.* (2003) obtained a total inventory of 47 Pg-C by using an ungridded GLODAP database. Using CFC data, Waugh *et al.* (2006) obtained a total inventory of 48 Pg-C. A comparative study using five long transoceanic cruises was performed by Vázquez-Rodríguez *et al.* (2009b). They found that φC_T° and *TrOCA* turn out 55 and 51 Pg-C respectively. The results obtained here with CARINA gridded showed the same integrated inventories as Vázquez-Rodríguez *et al.* (2009b) for the φC_T° method, but a higher value of 58 Pg-C for the *TrOCA* method. The main differences from the GLODAP gridded data (Lee *et al.*, 2003; Key *et al.*, 2004) are located in the South Atlantic, where a large number of GLODAP estimates (obtained from the ΔC^* method, Gruber *et al.*, 1996) are negative. The GLODAP values of C_{ANT} for the Southern Ocean are lower than the ones computed here. This negative bias in the C_{ANT} estimates from the GLODAP dataset has been identified by several authors (Lo Monaco *et al.*, 2005; Waugh *et al.*, 2006; Vázquez-Rodríguez *et al.*, 2009b). The discrepancies among the interpolation methods are rather low except in the upper layers and in the Southern Ocean (Fig. 6C). The *WMP* interpolation produces higher values of C_{ANT} than the spatial method in the deep Southern Ocean ($\theta < 5^\circ\text{C}$) and lower values in the upper layers where biases reach about $-8 \mu\text{mol kg}^{-1}$. In terms of C_{ANT} inventories the discrepancies are quite low and there are systematically lower (higher) values in the upper (lower) layer when the spatial interpolation is used (Table 2). The estimated total inventory of $\varphi C_T^\circ C_{ANT}$ for the Atlantic is 55 Pg-C, independently of the interpolation method applied. Nevertheless, some minor discrepancies are found when the warm and cold water (θ above or below the 5°C isotherm, respectively) inventories are examined separately (Table 2).

The above-described pattern is quite similar to the one obtained when the *TrOCA* method is used to estimate C_{ANT} . The total inventory does not change too

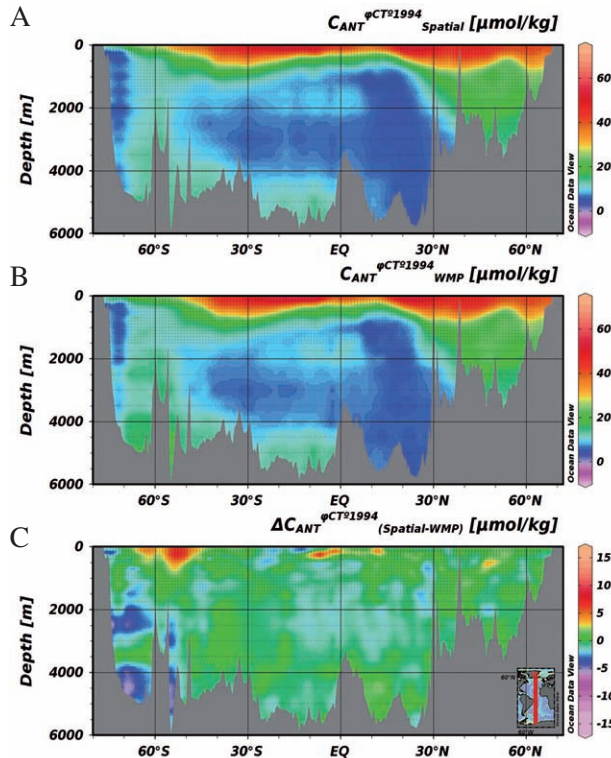


FIG. 6. – C_{ANT} ($\mu\text{mol kg}^{-1}$) determined by the ϕC_T° method along 28°W using spatial interpolation (A) and WMP interpolation (B). Residuals between the two interpolations are shown (C) as spatially interpolated minus WMP interpolated.

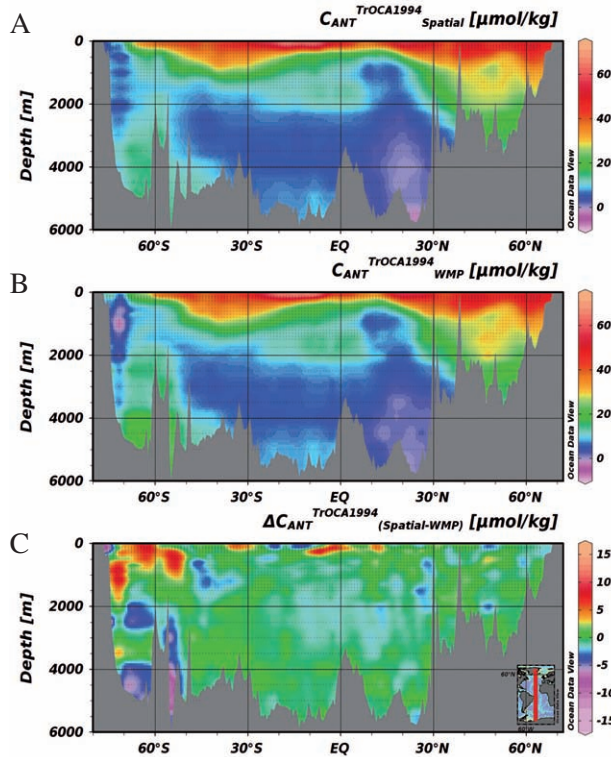


FIG. 7. – C_{ANT} ($\mu\text{mol kg}^{-1}$) determined by the $TrOCA$ method along 28°W using spatial interpolation (A) and WMP interpolation (B). Residuals between the two interpolations are shown (C) as spatially interpolated minus WMP interpolated.

TABLE 2. – C_{ANT} inventories (Pg-C) in the Atlantic and in different latitudinal bands and layers using the $TrOCA$ and ϕC_T° methods.

| C_{ANT} (Pg-C) 1994 Zone | $\theta(^{\circ}\text{C})$ | ϕC_T° | | | $TrOCA$ | | |
|-------------------------------|----------------------------|--------------------|------|------|---------|------|------|
| | | Spatial | WMP | diff | Spatial | WMP | diff |
| Lat>30°N | <5 | 6.9 | 7.0 | 0.1 | 8.1 | 8.1 | 0.0 |
| Lat>30°N | ≥ 5 | 6.0 | 5.8 | -0.2 | 6.7 | 6.5 | -0.2 |
| Tropical | <5 | 12.8 | 13.4 | 0.6 | 12.7 | 13.2 | 0.5 |
| Tropical | ≥ 5 | 10.2 | 9.7 | -0.5 | 10.5 | 9.9 | -0.6 |
| Lat<30°S | <5 | 15.5 | 16.3 | 0.8 | 15.9 | 16.7 | 0.8 |
| Lat<30°S | ≥ 5 | 3.7 | 3.1 | -0.6 | 4.0 | 3.2 | -0.8 |
| Atlantic Ocean | <5 | 35.2 | 36.7 | 1.4 | 36.6 | 38.0 | 1.4 |
| Atlantic Ocean | ≥ 5 | 19.9 | 18.6 | -1.3 | 21.2 | 19.6 | -1.7 |
| Total | | 55.1 | 55.2 | 0.1 | 57.9 | 57.6 | -0.2 |

much (roughly less than 5%, Table 2) when different interpolation methods are used, although the inventories in the warm and cold layers for the whole Atlantic Ocean are around 1.5 Pg-C different depending on the interpolation method used. Using the $TrOCA$ method produces a slightly higher C_{ANT} inventory. The $TrOCA$ method gives higher values in the surface layer (higher penetration) and in the deep Northern North Atlantic (Fig. 7). In comparison, the ϕC_T° method gives slightly higher values in practically all deep water masses and in the Southern Ocean, except for the Antarctic Bottom Water (AABW). Again, the major differences found in the southern latitudes are a consequence of the low density of carbon system data in this region.

Future work will be needed to improve the interpolation method and obtain an uncertainty assessment, and to iterate back and forth to the original data following a Barnes schema to fine-tune the interpolation. After these improvements have been achieved and with uncertainties available, the enhanced interpolation method could be used to interpolate the parameters available in CARINA and GLODAP, in order to provide an enhanced gridded product. Also, more C_{ANT} estimation techniques such as TTD and ΔC^* can be incorporated and applied to the CARINA database so that their inventories will be obtained.

CONCLUSIONS

The WMP interpolation method offers improvements compared with a traditional spatial gridding, and even with an objective analysis spatial gridding. By using an auxiliary database (WOA05) constructed with more resolution data on bio-geochemical conservative parameters, the WMP method has more information for the gridding task than any other exclusively spatial alternative.

The total inventory of C_{ANT} (referred to 1994) for the Atlantic Ocean is estimated to be about 55-58 Pg-C depending on the C_{ANT} estimation technique applied (ϕC_T° or $TrOCA$, respectively). The interpolation methods used here (spatial and WMP) do not have significant effects on the estimates of C_{ANT} total inventories, due to compensation effects between domains. Nevertheless, there exist some minor differences in the

results obtained by the different interpolation methods. The *WMP* interpolation method performs better than the spatial one, particularly in regions with less density of initial data (most importantly the Southern Ocean) from the CARINA dataset. Finally, the differences between the interpolation methods transcend to the realm of C_{ANT} estimation above and below the 5°C isopleth. The spatial method tends to produce lower (higher) C_{ANT} values in the water below (above) the isotherm of 5°C than the *WMP* interpolation method.

ACKNOWLEDGEMENTS

We would like to extend our gratitude to the chief scientists, scientists and crew who participated and offered their dedication to the oceanographic cruises used in this study. This work was developed and funded by the European Commission within the 6th Framework Programme (EU FP6 CARBOOCEAN Integrated Project, Contract no. 511176), MEC (CTM2006-27116-E/MAR) and by the Xunta de Galicia within the INCITE framework (M4AO project PGIDIT07PXB402153PR)

We also wish to thank the editor and the two anonymous reviewers, whose comments greatly contributed to improving and focusing the manuscript.

REFERENCES

- Anderson, L.A. and J.L. Sarmiento. – 1994. Redfield Ratios of Remineralization Determined by Nutrient Data Analysis. *Global Biogeochem. Cycles*, 8: 65-80.
- Antonov, J.I., R.A. Locarnini, T.P. Boyer, A.V. Mishonov, H.E. Garcia and S. Levitus. – 2006. World Ocean Atlas 2005, Volume 2: Salinity. S. Levitus. *NOAA Atlas NESDIS 62*, U.S. Government Printing Office, Washington, D.C.: 182.
- Bennett, A.F. – 1992. *Inverse methods in physical oceanography*. Cambridge University Press.
- Bretherton, F.P., R.E. Davis and C.B. Fandry. – 1976. A technique for objective analysis and design of oceanographic experiments applied to MODE-73. *Deep-Sea Res.*, 23: 559-582.
- Broecker, W.S. – 1974. “NO”, a conservative water-mass tracer. *Earth Planet. Sci. Lett.*, 23.
- Canadell, J.G., C. Le Quére, M.R. Raupach, C.B. Field, E.T. Buitenhuis, P. Ciais, T.J. Conway, N.P. Gillett, R.A. Houghton and G. Marland. – 2007. Contributions to accelerating atmospheric CO₂ growth from economic activity, carbon intensity, and efficiency of natural sinks. *Proc. Natl. Acad. Sci.*, 104: 18866.
- Emery, W.J. and R.E. Thomson. – 2001. *Data analysis methods in physical oceanography*. Elsevier Science.
- Freeland, H.J. and W.J. Gould. – 1976. Objective analysis of meso-scale ocean circulation features. *Deep-Sea Res.*, 23: 915-923.
- Gandin, L.S. and R. Hardin. – 1965. *Objective analysis of meteorological fields*. Israel program for scientific translations Jerusalem.
- Garcia, H.E., R.A. Locarnini, T.P. Boyer, J.I. Antonov and S. Levitus. – 2006a. World Ocean Atlas 2005, Volume 3: Dissolved Oxygen, Apparent Oxygen Utilization, and Oxygen Saturation. S. Levitus. *NOAA Atlas NESDIS 63*, U.S. Government Printing Office, Washington, D.C.: 342.
- Garcia, H.E., R.A. Locarnini, T.P. Boyer, J.I. Antonov and S. Levitus. – 2006b. World Ocean Atlas 2005, Volume 4: Nutrients (phosphate, nitrate, silicate). S. Levitus. *NOAA Atlas NESDIS 64*, U.S. Government Printing Office, Washington, D.C.: 396.
- Gruber, N., J.L. Sarmiento and T.F. Stocker. – 1996. An improved method for detecting anthropogenic CO₂ in the oceans. *Global Biogeochem. Cycles*, 10: 809-837.
- Hedges, J.I., W.A. Clark and G.L. Cowie. – 1988. Organic matter sources to the water column and superficial sediments of a marine bay. *Limnol. Oceanogr.*, 33: 1116-1136.
- Heinze, C. – 2004. Simulating oceanic CaCO₃ export production in the greenhouse. *Geophys. Res. Lett.*, 31: L16308.
- Hoppema, M., A. Velo, S. van Heuven, T. Tanhua, R.M. Key, X. Lin, D.C.E. Bakker, F.F. Pérez, A.F. Ríos, C. Lo Monaco, C.L. Sabine, M. Alvarez and R.G.J. Bellerby. – 2009. Consistency of cruise data of the CARINA database in the Atlantic sector of the Southern Ocean. *Earth Syst. Sci. Data*, 1: 63-75.
- Jalilickee, J.B. and D.R. Hamilton. – 1977. Objective analysis and classification of oceanographic data. *Tellus*, 29.
- Joos, F., G.K. Plattner, T.F. Stocker, O. Marchal and A. Schmittner. – 1999. Global warming and marine carbon cycle feedbacks on future atmospheric CO₂. *Science*, 284: 464.
- Key, R.M., A. Kozyr, C.L. Sabine, K. Lee, R. Wanninkhof, J.L. Bullister, R.A. Feely, F.J. Millero, C. Mordy and T.H. Peng. – 2004. A global ocean carbon climatology: Results from Global Data Analysis Project (GLODAP). *Global Biogeochem. Cycles*, 18, GB4031.
- Key, R.M., T. Tanhua, A. Olsen, M. Hoppema, S. Jutterström, C. Schirnick, S. van Heuven, A. Kozyr, X. Lin, A. Velo, D.W.R. Wallace and L. Mintrop. – 2010. The CARINA data synthesis project: Introduction and overview. *Earth Syst. Sci. Data*, 2: 105-121.
- Kortzinger, A., J.I. Hedges and P.D. Quay. – 2001. Redfield ratios revisited: Removing the biasing effect of anthropogenic CO₂. *Limnol. Oceanogr.*, 964-970.
- Le Quére, C., C. Rodenbeck, E.T. Buitenhuis, T.J. Conway, R. Langenfelds, A. Gomez, C. Labuschagne, M. Ramonet, T. Nakazawa and N. Metzl. – 2007. Saturation of the Southern Ocean CO₂ sink due to recent climate change. *Science*, 316: 1735.
- Lee, K., S.D. Choi, G.H. Park, R. Wanninkhof, T.H. Peng, R.M. Key, C.L. Sabine, R.A. Feely, J.L. Bullister and F.J. Millero. – 2003. An updated anthropogenic CO₂ inventory in the Atlantic Ocean. *Global Biogeochem. Cycles*, 17: 1116.
- Lo Monaco, C., C. Goyet, N. Metzl, A. Poisson and F. Touratier. – 2005. Distribution and inventory of anthropogenic CO₂ in the Southern Ocean: Comparison of three data-based methods. *J. Geophys. Res.*, 110: 9.
- Locarnini, R.A., A.V. Mishonov, J.I. Antonov, T.P. Boyer, H.E. Garcia and S. Levitus. – 2006. World Ocean Atlas 2005, Volume 1: Temperature. S. Levitus. *NOAA Atlas NESDIS 61*, U.S. Government Printing Office, Washington, D.C.: 182.
- Matear, R.J., C.S. Wong and L. Xie. – 2003. Can CFCs be used to determine anthropogenic CO₂? *Global Biogeochem. Cycles*, 17: 1013.
- Mémery, L., M. Arhan, X.A. Alvarez-Salgado, M.J. Messias, H. Mercier, C.G. Castro and A.F. Ríos. – 2000. The water masses along the western boundary of the south and equatorial Atlantic. *Progr. Oceanogr.*, 47: 69-98.
- Pérez, F.F., C. Mourino, F. Fraga and A.F. Ríos. – 1993. Displacement of water masses and remineralization rates off the Iberian Peninsula by nutrient anomalies. *J. Mar. Res.*, 51: 869-892.
- Ríos, A.F., F. Fraga and F.F. Pérez. – 1989. Estimation of coefficients for the calculation of “NO”, “PO” and “CO”, starting from the elemental composition of natural phytoplankton. *Sci. Mar.*, 53: 779-784.
- Sabine, C.L., R.M. Key, K.M. Johnson, F.J. Millero, A. Poisson, J.L. Sarmiento, D.W.R. Wallace and C.D. Winn. – 1999. Anthropogenic CO₂ inventory of the Indian Ocean. *Global Biogeochem. Cycles*, 13: 179-198.
- Sabine, C.L., R.A. Feely, N. Gruber, R.M. Key, K. Lee, J.L. Bullister, R. Wanninkhof, C.S. Wong, D.W.R. Wallace and B. Tilbrook. – 2004. The oceanic sink for anthropogenic CO₂. *Science*, 305: 367-371.
- Tanhua, T., A. Olsen, M. Hoppema, S. Jutterström, C. Schirnick, S. Van Heuven, A. Velo, X. Lin, A. Kozyr, M. Alvarez, D.C.E. Bakker, P. Brown, E. Falck, E. Jeansson, C. Lo Monaco, J. Olafsson, F.F. Pérez, D. Pierrot, A.F. Ríos, C.L. Sabine, U. Schuster, R. Steinfeldt, I. Stendardo, L.G. Anderson, N.R. Bates, R.G.J. Bellerby, J. Blindheim, J.L. Bullister, N. Gruber, M. Ishii, T. Johannessen, E.P. Jones, J. Köhler, A. Kortzinger, N. Metzl, A. Murata, S. Musielewicz, A.M. Omar, K.A. Olsson, M. de la Paz, B. Pfeil, F. Rey, M. Rhein, I. Skjelvan, B. Tilbrook, R. Wanninkhof, L. Mintrop, D.W.R. Wallace and R.M. Key. – 2009. CARINA Data Synthesis Project. *ORNL/CDIAC-157, NDP-091, Carbon Dioxide Information Analysis Center, Oak Ridge National Laboratory, U.S. Department of Energy, Oak Ridge, Tennessee, 37831-6335*.

- Tanhua, T., R. Steinfeldt, R.M. Key, P. Brown, N. Gruber, R. Wanninkhof, F.F. Pérez, A. Körtzinger, A. Velo, U. Schuster, S. van Heuven, J.L. Bullister, I. Stendardo, M. Hoppema, A. Olsen, A. Kozyr, D. Pierrot, C. Schirnick and D.W.R. Wallace. – 2010. Atlantic Ocean CARINA data: overview and salinity adjustments. *Earth Syst. Sci. Data*, 2: 17-34.
- Thomas, H. and V. Ittekkot. – 2001. Determination of anthropogenic CO₂ in the North Atlantic Ocean using water mass ages and CO₂ equilibrium chemistry. *J. Mar. Syst.*, 27: 325-336.
- Touratier, F., L. Azouzi and C. Goyet. – 2007. CFC-11, $\Delta^{14}\text{C}$ and ^3H tracers as a means to assess anthropogenic CO₂ concentrations in the ocean. *Tellus B*, 59: 318-325.
- U.S. Department of Commerce, N.O.a.A.A., National Geophysical Data Center. – 2006. *2-minute Gridded Global Relief Data (ETOPO2v2)*.
- Vázquez-Rodríguez, M., X.A. Padin, A.F. Ríos, R.G.J. Bellerby and F.F. Pérez. – 2009a. An upgraded carbon-based method to estimate the anthropogenic fraction of dissolved CO₂ in the Atlantic Ocean. *Biogeosci. Discuss.*, 6: 4527-4571.
- Vázquez-Rodríguez, M., F. Touratier, C. Lo Monaco, D.W. Waugh, X.A. Padin, R.G.J. Bellerby, C. Goyet, N. Metzl, A.F. Ríos and F.F. Pérez. – 2009b. Anthropogenic carbon distributions in the Atlantic Ocean: data-based estimates from the Arctic to the Antarctic. *Biogeosciences*, 6: 439-451.
- Waugh, D.W., T.M. Hall, B.I. McNeil, R. Key and R.J. Matear. – 2006. Anthropogenic CO₂ in the oceans estimated using transit time distributions. *Tellus B*, 58: 376-389.

Received November 1, 2008. Accepted July 26, 2010.

Published online November 13, 2010.